

The University of Akron

IdeaExchange@UAkron

Williams Honors College, Honors Research
Projects

The Dr. Gary B. and Pamela S. Williams Honors
College

Spring 2023

Comparing Weathering Effects of Ultraviolet and Xenon Arc Accelerated Aging on Polyvinyl Chloride

Collin McInnes
ccm57@uakron.edu

Follow this and additional works at: https://ideaexchange.uakron.edu/honors_research_projects



Part of the [Polymer and Organic Materials Commons](#), and the [Polymer Science Commons](#)

Please take a moment to share how this work helps you [through this survey](#). Your feedback will be important as we plan further development of our repository.

Recommended Citation

McInnes, Collin, "Comparing Weathering Effects of Ultraviolet and Xenon Arc Accelerated Aging on Polyvinyl Chloride" (2023). *Williams Honors College, Honors Research Projects*. 1744.

https://ideaexchange.uakron.edu/honors_research_projects/1744

This Dissertation/Thesis is brought to you for free and open access by The Dr. Gary B. and Pamela S. Williams Honors College at IdeaExchange@UAkron, the institutional repository of The University of Akron in Akron, Ohio, USA. It has been accepted for inclusion in Williams Honors College, Honors Research Projects by an authorized administrator of IdeaExchange@UAkron. For more information, please contact mjon@uakron.edu, uapress@uakron.edu.

Executive Summary

The ever-growing presence of polymers has seen large amounts of plastic materials used in outdoor applications where they are exposed to the elements constantly, including ultraviolet radiation and high levels of moisture. Multiple accelerated aging methods exist to mimic the effects of long-term exposure to moisture and sunlight but do so utilizing different wavelengths of the sunlight spectrum to instigate polymer deterioration. This study aims to analyze how polyvinyl chloride (PVC) ages differently when exposed to either strictly ultraviolet (UV) radiation, or full sunlight spectra simulation via a xenon arc lamp.

To do this, a 1006-hour cycle was developed on both a QUV/spray unit and Q-SUN Xe-1 unit, with 672 hours of uninterrupted dry light exposure, immediately followed by 336 hours of an alternating wet/dry cycle where the samples would be exposed to intermittent periods of moisture treatment. All samples were entered together, and some were taken out at designated progress points—around 167 hours—throughout the aging process until a set of samples existed for every 167-hour interval for each unit. These samples were then analyzed for cosmetic changes via digital photography and colorimetry, chemical changes via thermogravimetric analysis (TGA) and Fourier transform infrared spectrometry (FT-IR), and mechanical changes via dynamic mechanical analysis (DMA).

These analyses showed that UV-exposed samples showed significantly more discoloration than the xenon-exposed samples—CIELAB color space analysis yielded ΔE values up to 11 for dry aging and up to 37 for wet/dry aging, while xenon-exposed samples never had ΔE values higher than 5. For the other forms of analysis, the samples showed similar characteristics with respect to the control PVC. TGA revealed a lower T_d and % residue for the samples that had seen 503 or 672 hours of solely dry aging compared to all other progress points

for both exposure forms. Also, new FT-IR peaks presented at 3300 cm^{-1} and 1600 cm^{-1} after wet/dry treatment and all samples tested showed stiffer behavior than the control sample. However, for both of these cases, the UV-exposed samples demonstrated these traits more severely—the FT-IR peaks of the UV-exposed samples were all stronger than the xenon-exposed samples, and the UV-exposed samples showed stiffer performance than their xenon-exposed counterparts. Additionally, the variation in the DMA curves was much larger than that of the xenon-exposed samples—the UV-exposed samples had ranges of up to 2 GPa at 85°C , while the xenon-exposed samples only varied .27 GPa at 85°C . Thus, it can be concluded that strictly UV exposure causes stronger colorant deterioration, and stronger albeit less consistent chemical deterioration and mechanical changes than xenon-arc spectrum aging.

Designing and executing this experiment elevated my ability to utilize multiple sources information to create a new procedure on two different machines meant to give identical treatment to samples. Additionally, I gained invaluable experience learning how to operate a controlled experiment in a busy, industrial environment where external factors can create sudden changes that must be dealt with.

Future work could include studying the aging effects of these cycles on different polymers to see how the inherent spectra differences manifest on other commonly exposed materials such as high-density polyethylene, as well as analyzing how closely the accelerated aged samples compared to materials naturally aged.

Introduction

The degradation of polymers has become an area of intense focus in the past decades, especially as unprecedented amounts of polymer waste are sent to landfills and into oceans where they degrade and break down when exposed to the elements, leaking into ecosystems. At the current production rate, it is estimated that 12 billion metric tons of plastic waste will have gone to landfill by 2050 [4]. Thus, being able to simulate the effects of long-term aging on an accelerated timescale is vital to understanding and combating the presence of plastic waste. Additionally, accurate accelerated aging is also needed to simulate plastic product lifespans and their usefulness in environmental applications.

Polyvinyl chloride (PVC) is a widely used polymer compound, present in a vast array of industries including construction, automotive, and healthcare [7]. Due to its pervasiveness in daily life, particularly in ways that come in contact with humans, studies have been performed to examine the aging effects of rigid PVC [6], plasticized PVC—which is commonly used in medical settings [1]—and PVC microplastics [2]. Additionally, work has been done to examine how accelerated aging techniques compare to natural outdoor aging [3]. With that in mind, it would be valuable to have data to show how accelerated aging methods compare to one another for future studies to be able to refer to in order to decide which method best suits their specific needs.

Background

PVC is a halogenated polyolefin synthesized from emulsion polymerization. Its chemical structure is shown in **Figure 1**. It is noted for its excellent durability, particularly its resistance to abrasion and scratches, as well as its processability—it is able to be plasticized to be rubbery or reinforced to be rigid. Due to this processability, PVC can be utilized in a wide range of

applications, ranging from synthetic rubber to outdoor fence posts. These rigid outdoor applications are high-volume and long-lasting in the environment and readily recycled when in pure form.

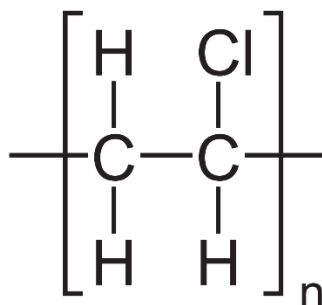


Figure 1: Chemical structure of polyvinyl chloride (PVC)

There are many common machines utilized to perform accelerated aging on polymer materials; this study will focus on two of them. The first is a QUV/spray unit, which utilizes fluorescent ultraviolet (UV) lights to simulate specifically the UV portion of the sunlight spectrum, as the UV spectrum is noted to be a highly damaging portion of the sunlight spectrum [11]. The second is a Q-SUN Xe-1 unit, which utilizes electrified ionized xenon to create light that can be further filtered to fully simulate the entire sunlight spectrum. Despite these differences in spectrum, these methods have been used interchangeably both in industry and in literature to simulate aging [1,2,3]. Studying these methods to see if they have inherent differences, particularly on materials commonly exposed to moisture and sunlight, would be of use for future studies to decide which method is more suited to their means.

For this study, samples will be subjected to a long-term accelerated aging cycle, with some samples procedurally being removed from the chambers to document progress points in the aging process. The samples would then be measured for cosmetic changes via colorimetry and digital photography, chemical changes via thermogravimetric analysis (TGA) and Fourier

transform infrared spectroscopy (FT-IR), and mechanical integrity via dynamic mechanical analysis (DMA).

Experimental Methods

In order to ensure that both samples would be exposed to the same amount of aging in each chamber and be exposed long enough to exhibit significant deterioration, a test procedure needed to be designed. Utilizing ASTM testing standards D4329-99, G154-06 and G155-05a as a guide [8,9,10] in conjunction with established industry practice at Quanex Corporation, with whom this project is performed in collaboration with, a 1008-hour process was designed for both units. This process involved a 672-hour (4-week) “dry” cycle, where no moisture was added to the machine, and a subsequent 336-hour (2-week) “wet/dry” cycle, where samples would alternate between further dry treatment and moisture treatment. For both machines, the dry cycle was set to a constant exposure of $0.55 \text{ W/m}^2/\text{nm}$ at 60°C . For the wet/dry cycle, the two chambers were set to a two-step loop. For the QUV unit, this loop consisted of 8 hours of UV exposure at $0.55 \text{ W/m}^2/\text{nm}$ at 60°C , followed by 4 hours of condensation exposure from a heated reverse osmosis (RO) water bath at 50°C , with the UV lamps turned off. For the Q-SUN chamber, the samples were exposed to 102 minutes of light at $0.55 \text{ W/m}^2/\text{nm}$ at 63°C , followed by 18 minutes of light exposure at $0.55 \text{ W/m}^2/\text{nm}$ at 63°C while being sprayed by RO water via nozzles.

The specific material utilized in this study was the Quanex “Universal Formulation” (UF) PVC. The UF PVC material was cut into samples approximately 13–20 mm wide, 100 mm long, and 2 mm thick as measured via calibrated calipers. All samples were then measured for colorimeter values before being exposed to any aging.

For the QUV unit, the PVC samples were placed into specimen holders mounted with an aluminum backplate and snap-action mounters. The PVC samples were longer than the specimen holder windows to be able to stay fixed in the holder, so only the area exposed to the UV light was considered for further testing. Each specimen holder with PVC samples would then be loaded into the UV chamber with one blank holder in between. When samples would be unloaded, the specimen holders would be rotated as shown in **Figure 2** and described in ASTM standard G154-06 [9].



Figure 2: Schematic of the rotation pattern followed for QUV/spray chamber. Samples removed for data collection were taken from left to right, and sample holders without samples were filled with blanks.

For the xenon chamber, the samples were all placed onto the specimen tray loosely before the machine would run. Upon unloading a subset, the remaining samples would be moved in a clockwise fashion to allow for even exposure, as shown in **Figure 3**. Note that for both samples, only one “face” of the sample was exposed and was thus the only side analyzed.



Figure 3: Schematic of rotation pattern followed for Q-SUN Xe-1 unit. Samples removed for data collection were taken from left to right. While this rotation schedule was followed for these sections of the testing tray, exact positioning of the samples was not monitored.

A subset of 3 individual samples would be removed from each chamber roughly every 167 hours to represent a progress point. These progress points were denoted as “weeks,” as each subset was removed from treatment roughly 7 days apart. These samples would be immediately photographed and measured for colorimetry data, then stored in a sealed bag away from any light and moisture for further testing. This process would be continued on both machines every 167 hours until the entire 1008 hours had elapsed, leading to 12 total subsets of samples. Details of the exact amount of exposure sustained for these samples are summarized in **Table 1**.

Table 1: Summary of exact amounts of treatment provided to all subsets of tested samples.

Week #	UV	Xenon
1	167 hours of dry cycle	168 hours of dry cycle
2	335 hours of dry cycle	335 hours of dry cycle
3	503 hours of dry cycle	504 hours of dry cycle
4	Full dry cycle (672 hours)	Full dry cycle (672 hours)
5	Full dry cycle, plus 135 hours of wet/dry cycle	Full dry cycle, plus 106 hours of wet/dry cycle (778 hours total)
6	Full dry cycle, ~200 hours of wet/dry cycle, and 212 hours of alternate cycle (4 hours UV @ 0.77 W/m ² /nm at 60°C, 4 hours condensation at 48°C)	Full dry and wet/dry cycle (1008 hours total)

Immediately after being removed from exposure, a portion of each sample that appeared the most visibly discolored would be measured for colorimetry values with a calibrated X-Rite Ci6x colorimeter utilizing the CIELAB space. In all samples taken out during the dry cycle, any discoloration was uniform; thus, a spot was chosen at random to measure color data. For the wet/dry cycle, aging was not uniform; therefore, a spot that represented the most discoloration was chosen to represent the “worst case” scenario for that process. The samples were then scanned for IR spectra using a Perkin Elmer Frontier spectrometer equipped with an attenuated total reflection (ATR) system. One sample then had approximately 2mg of exposed material removed from its surface, and run for TGA, wherein the sample was heated from 30 to 600°C at 20°C/min, then from 600 to 900°C at 5°C/min. Due to a TGA’s ability to reveal material composition, full TGA curves are not disclosed in this report; instead, the thermal decomposition temperature (T_d) measured at 95 wt.% remaining, as well as the % residue of each sample were recorded. Finally, another sample from each subset was cut to 60mm long and 12mm wide for DMA testing utilizing a dual cantilever clamp on a TA Instruments DMA 850. A strain sweep was performed on the control sample to determine the best strain amount for the DMA, which

was determined to be 10 μ m. Then, the DMA was run from 15 to 125°C at a 5°C/min ramp rate, during which the storage and loss modulus were measured, as well as tan delta.

Results

Throughout the extent of the aging process, the UV-exposed samples were consistently noticeably more discolored and yellowed than the xenon-exposed samples for every progress point as shown in **Figure 4**. This difference became drastic once the wet/dry cycle was introduced; the UV-exposed samples showed significant browning and splotching due to the water condensing on its surface, while the xenon-exposed samples continued to only yellow slightly and uniformly even with the addition of moisture spray. This visual change is corroborated with the colorimeter values in **Figure 5**. Delta E values for the UV-exposed samples slowly increased from 2.44 ± 0.37 in Week 1 to a maximum of 9.91 ± 1.11 in Week 4, only to sharply increase to 35.4 ± 1.92 once water was introduced in Week 5. However, xenon only hit a maximum of 3.88 ± 0.56 , which was in Week 4. For **Figure 5**, Delta E values for the change in color were determined using the dE76 formula.

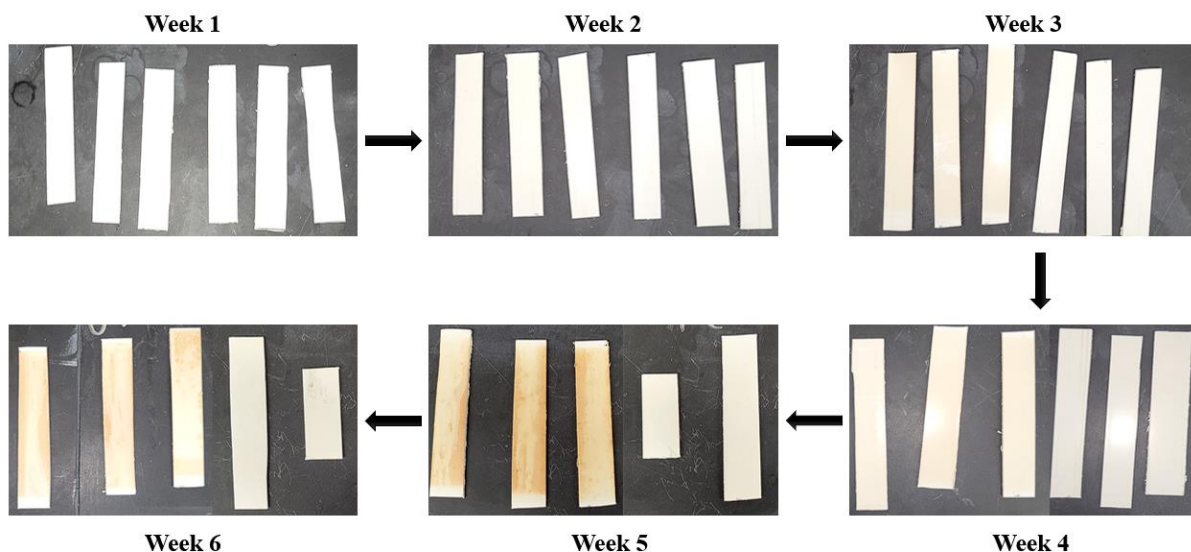


Figure 4: Digital images comparing discoloring of UV vs. xenon aged samples via digital photography. In all images above, UV samples are on the left and xenon samples are on the right.

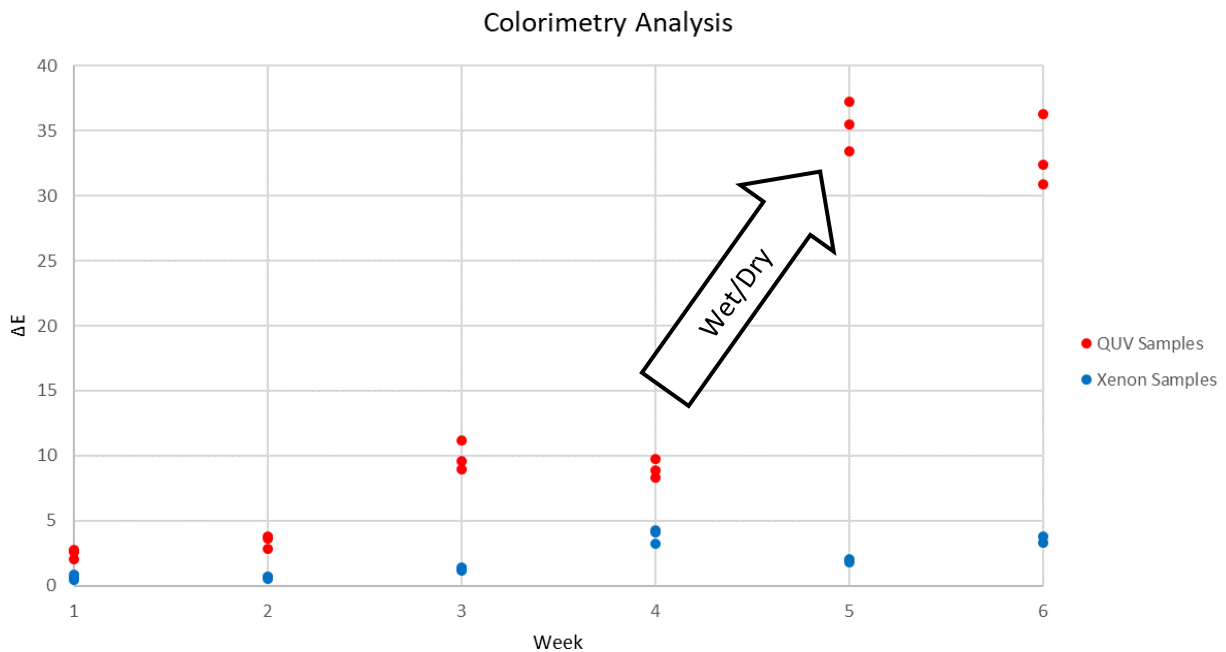


Figure 5: The ΔE values for each sample compared to their original $L^*a^*b^*$ values are plotted above. The UV aged samples are above the xenon-aged samples in every group, and the UV-aged samples jump precipitously from Week 4 to 5, when the moisture treatment is added, as indicated by the arrow.

While full TGA curves are not disclosed, it can be noted that analysis of these curves showed characteristic loss of HCl in all 13 samples run. As shown in **Figure 6**, both exposure methods had consistent T_g and % residue values for their initial dry and wet/dry cycle measurements – all T_g s for these points were between 290 and 296°C, and % residues ranged from 7.96% to 8.53%. However, these values decreased for both exposure methods for Weeks 3 and 4— T_g s for these weeks ranged from 278 to 283°C, and % residue dipped as low as 0.74% for Week 3 of the UV-exposed samples.

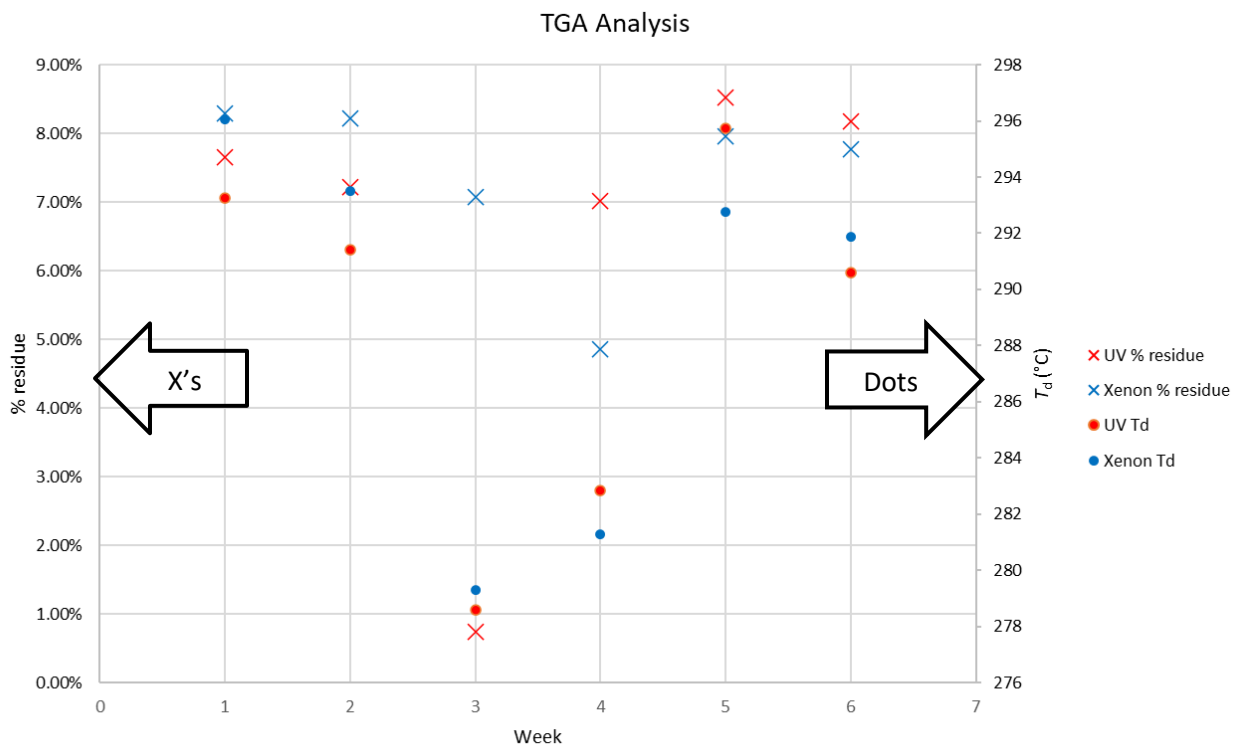


Figure 6: % residue and T_d at 95 wt% is plotted above for each week and each aging type.

FT-IR spectrometry revealed two areas where spectra differed in later aging: two wide peaks, one near 3400 cm^{-1} and another near 1600 cm^{-1} for Weeks 5 and 6 of the UV-exposed samples and Week 6 of the xenon-exposed samples. Spectra for these noted areas are shown in **Figures 7-10**.

UV FT-IR Section 1

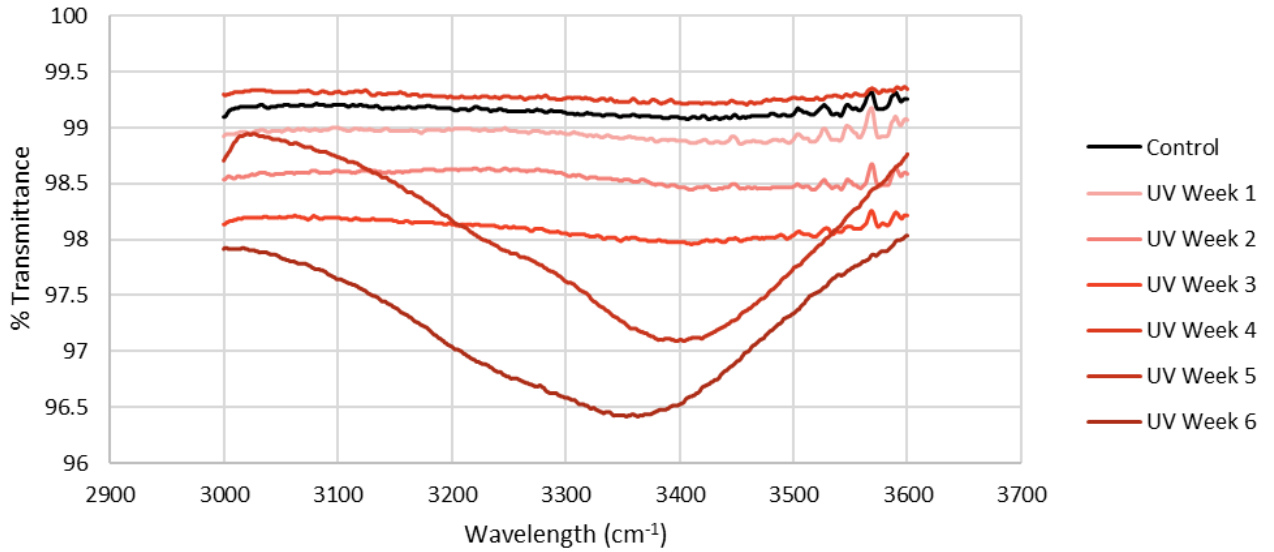


Figure 7: FT-IR spectrometry results for all UV-aged samples from wavelength 3000 cm^{-1} to 3600 cm^{-1} , as well as control data. The peaks present for Week 5 and Week 6 indicate the presence of water and/or hydrolyzed chlorines.

Xenon FT-IR Section 1

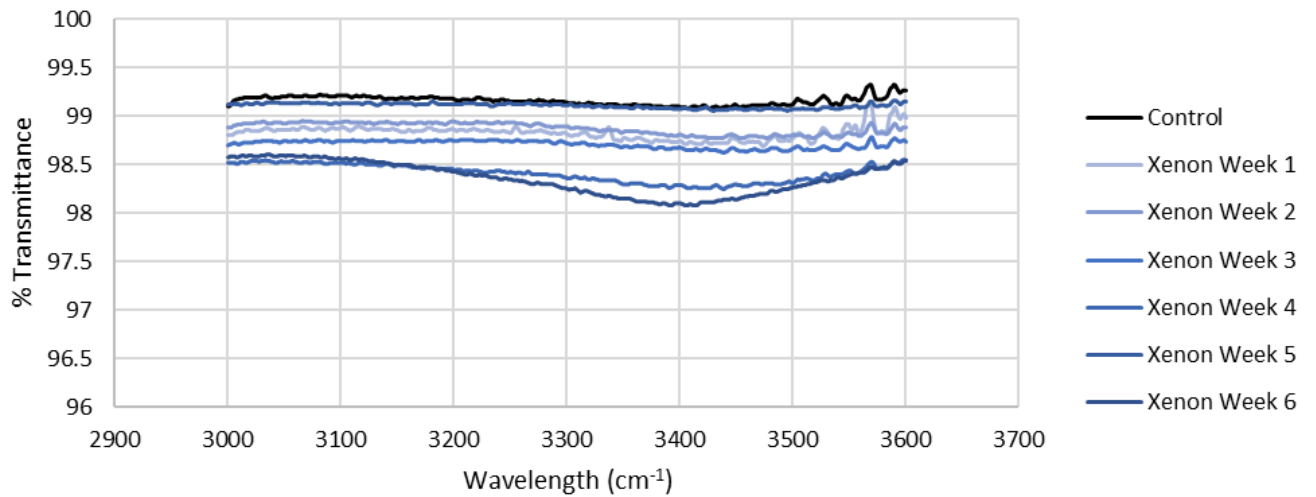


Figure 8: FT-IR spectrometry results for all xenon-aged samples from wavelength 3000 cm^{-1} to 3600 cm^{-1} , as well as control data. The peak present for Week 6 indicates the presence of water and/or hydrolyzed chlorines.

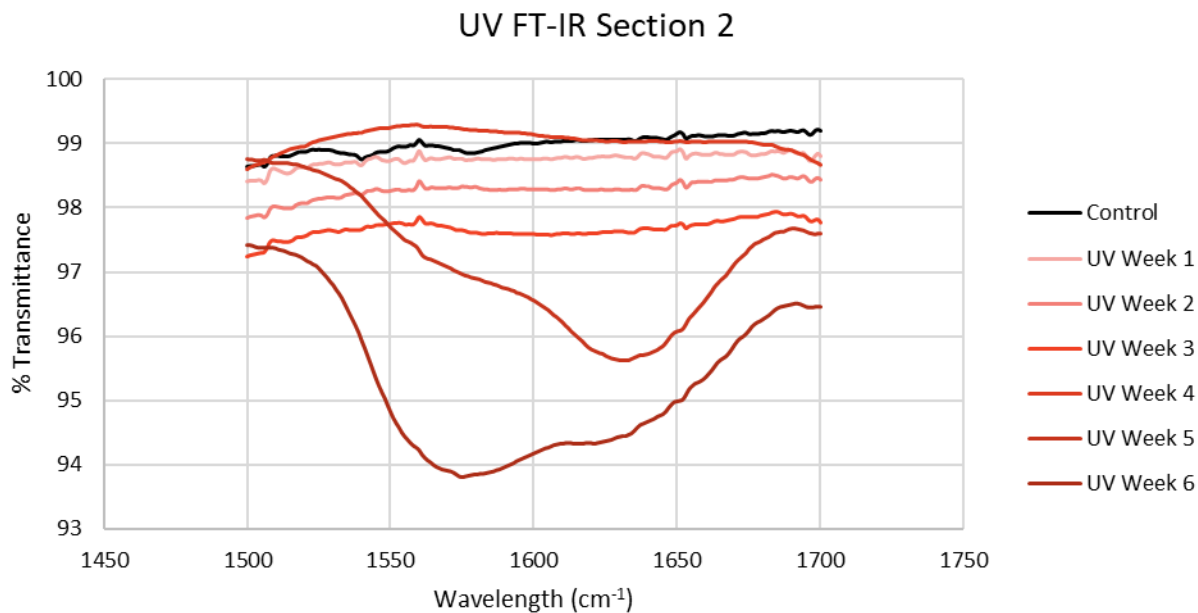


Figure 9: FT-IR spectrometry results for all UV-aged samples from wavelength 1500 cm⁻¹ to 1700 cm⁻¹, as well as control data. The peaks for Weeks 5 and 6 indicate alkene bonds, which would present after elimination of chlorines in the polymer backbone.

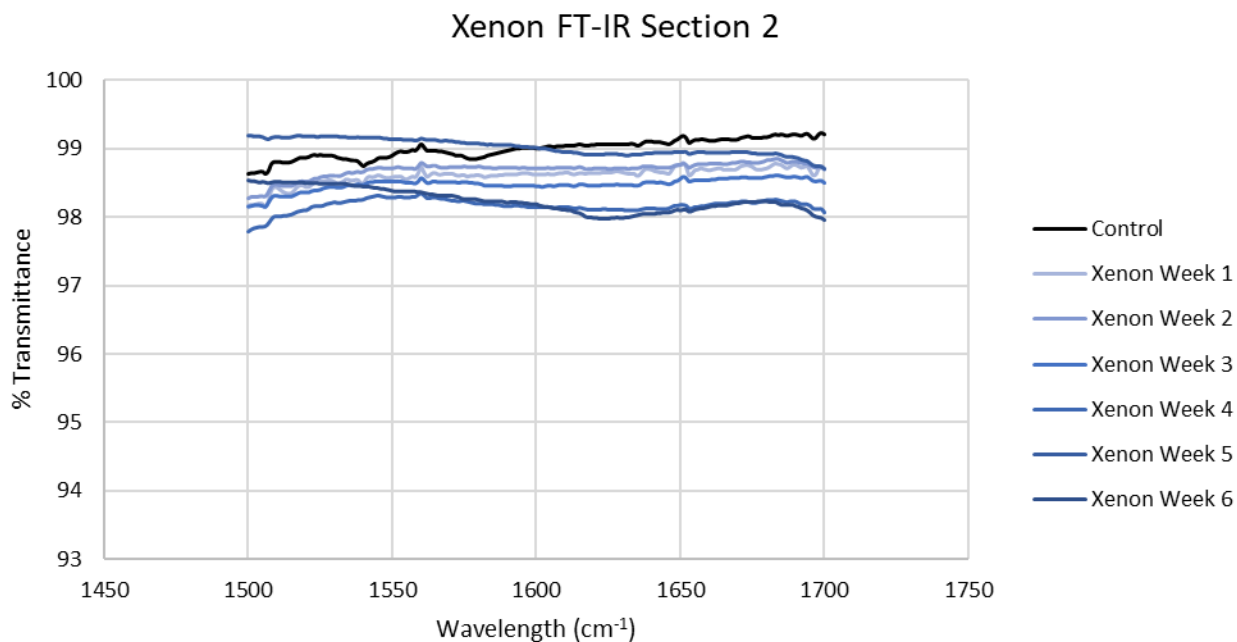


Figure 10: FT-IR spectrometry results for all xenon-aged samples from wavelength 1500 cm⁻¹ to 1700 cm⁻¹, as well as control data. The peak for Week 6 indicates alkene bonds, which would present after elimination of chlorines in the polymer backbone.

The DMA analysis showed consistent curves with similar mechanical stiffness, but with two main areas of variance: the loss moduli of the glassy region and the storage moduli above the glass transition temperature. In both these regions, while there was no apparent correlation between total modulus and the amount of aging exposure, the UV-exposed samples showed more variance than the xenon-exposed for both regions. Additionally, the control was the least stiff sample of all 13 samples tested, showing the precipitous storage modulus decrease a full 8°C earlier than any of the UV-exposed samples. Full curves are shown in **Figures 11-14**.

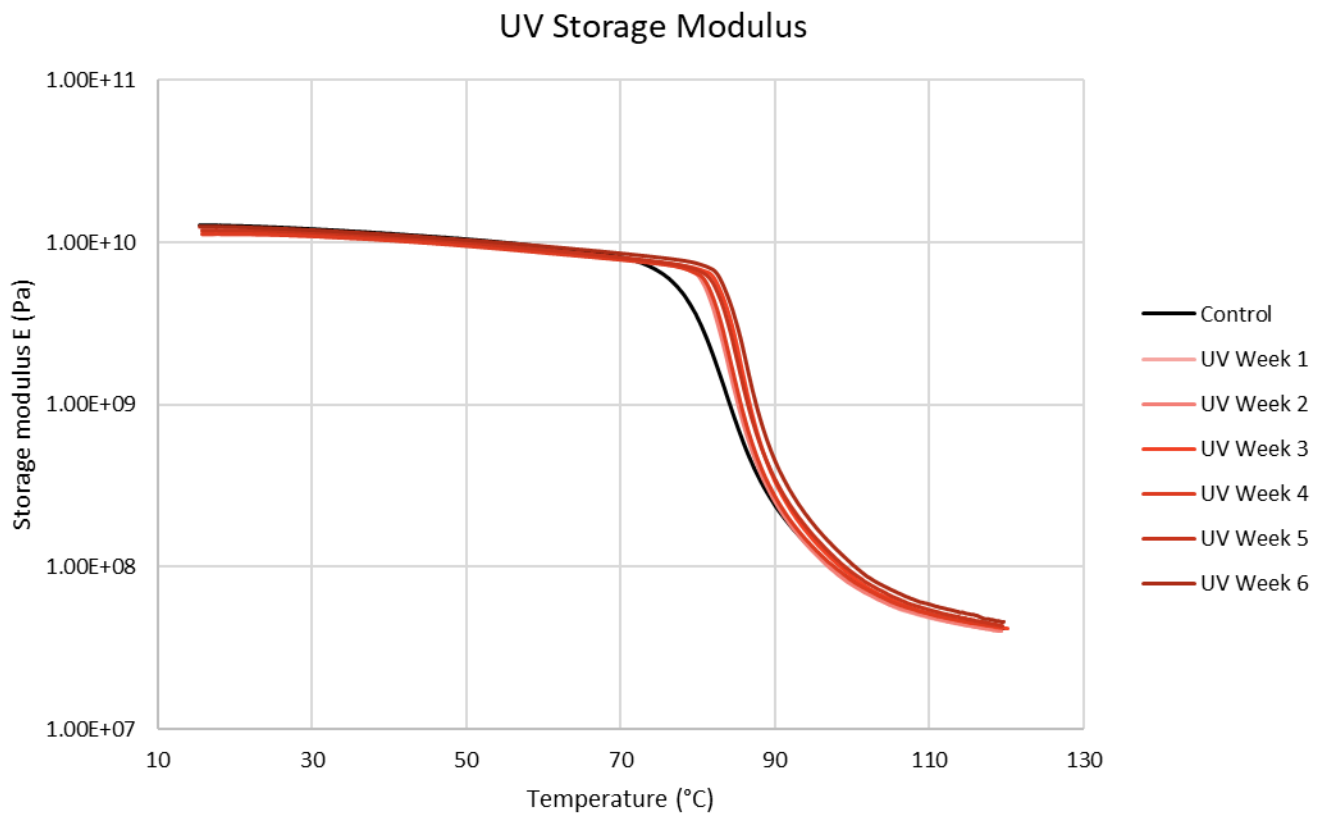


Figure 11: Storage modulus from 15–125°C of all UV-aged samples. Modulus is measured on a logarithmic scale.

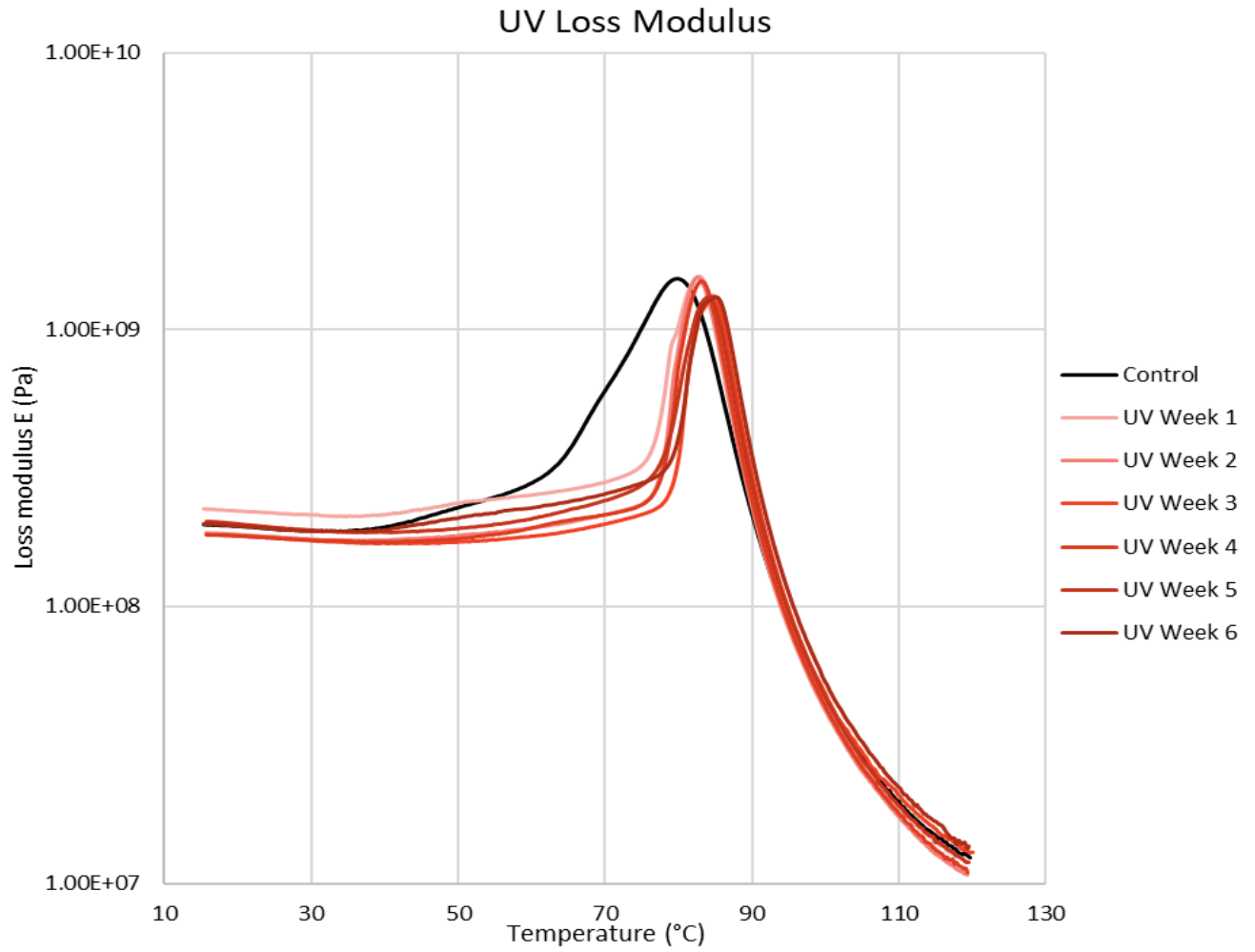


Figure 12: Loss modulus from 15–125°C of all UV-aged samples. Modulus is measured on a logarithmic scale.

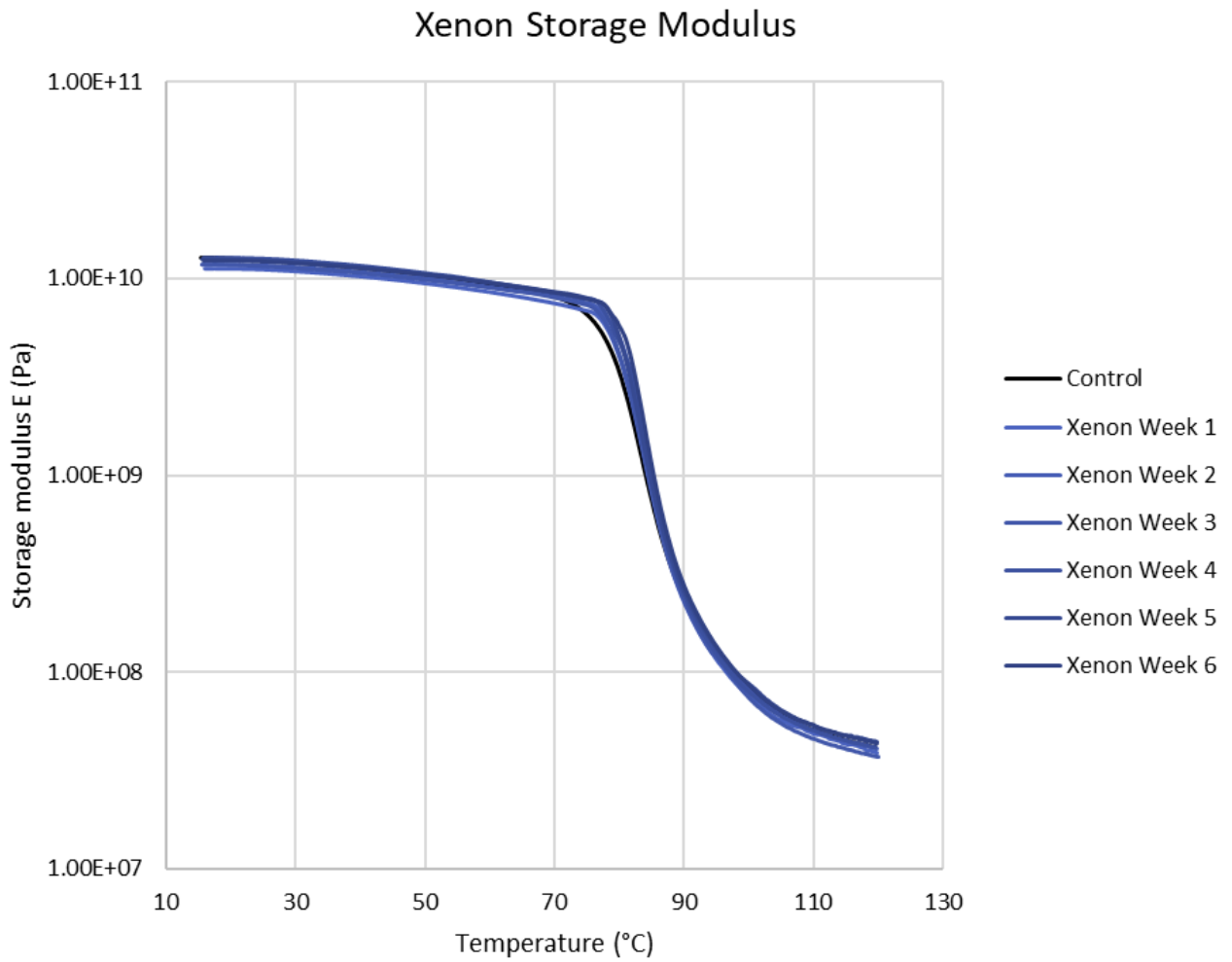


Figure 13: Storage modulus from 15–125°C of all xenon-aged samples. Modulus is measured on a logarithmic scale.

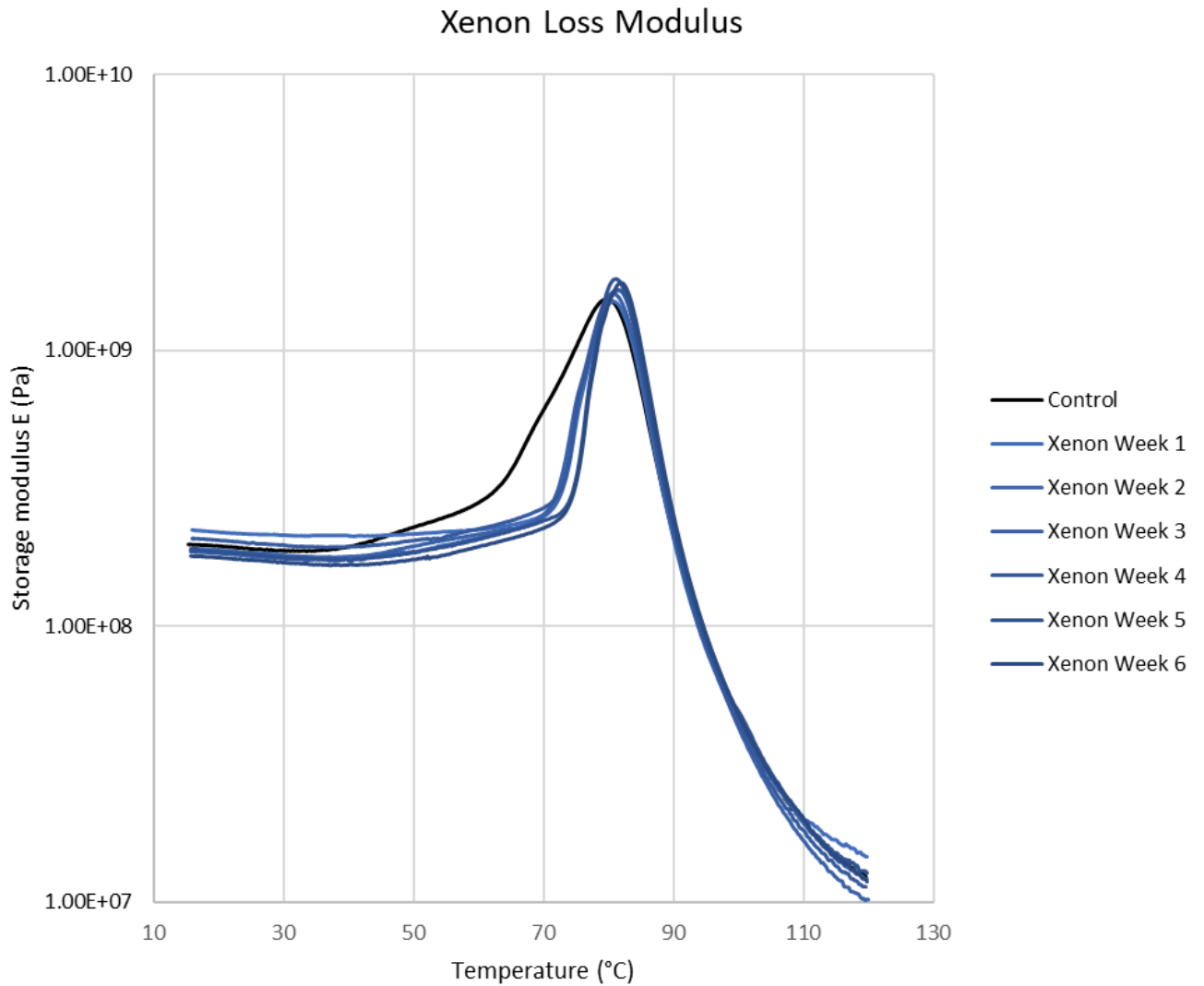


Figure 14: Loss modulus from 15–125°C of all xenon-aged samples. Modulus is measured on a logarithmic scale.

Additionally, analysis of T_g showed that glass transition temperature for the xenon-exposed samples stayed moderately consistent, with all values between 86.5 and 87.5°C and no consistent trend. The UV-exposed samples had more variation and generally increased with more exposure, rising from 87.24°C in Week 4 to 88.72°C in Week 6, as seen in **Figure 15**.

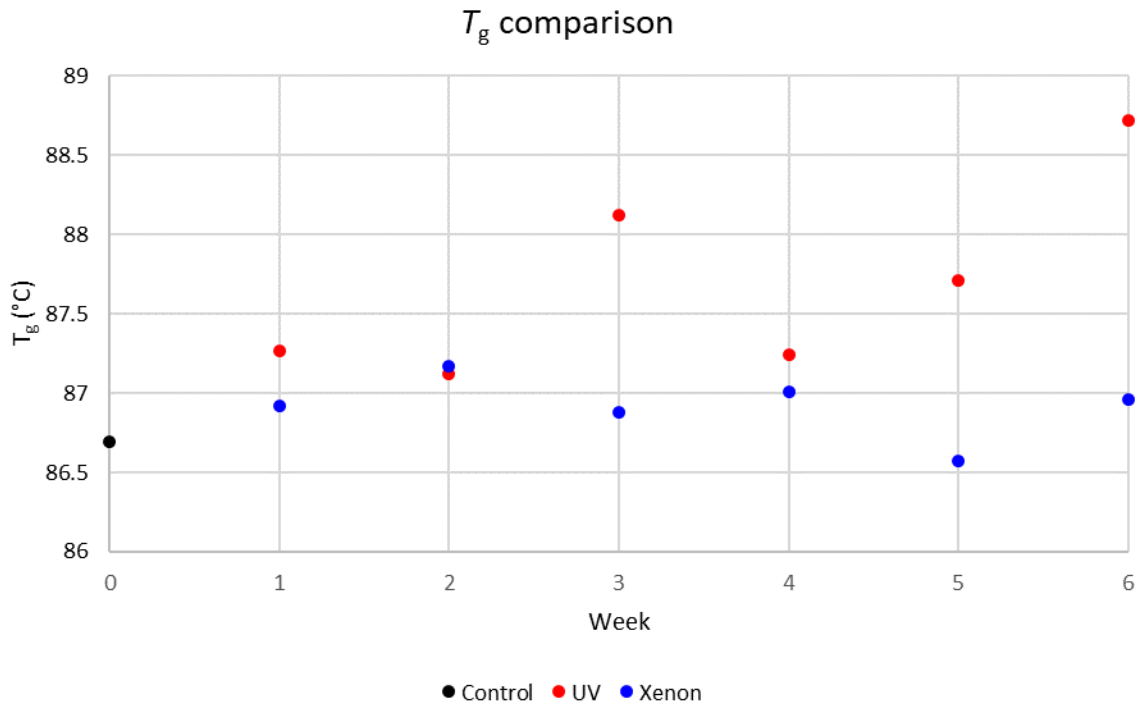


Figure 15: T_g of UV and xenon aged samples for each week of aging exposure. T_g was determined from the temperature at which tan delta was at maximum during DMA testing.

Discussion

The largest difference observed between the two exposure types was cosmetic. The UV-exposed samples discolored significantly more than the xenon-exposed samples, especially after moisture exposure, despite the cycles being designed to expose both sets to the exact same amount of irradiation and moisture. This discrepancy is likely due to the differences wavelengths at which the chambers emit radiation—the QUV is singularly focused on emitting the short-wave UV radiation portion of the sunlight spectrum, so materials with colorants more susceptible to short-wave UV degradation are likely to appear more yellowed or browned in the QUV chamber than the Q-SUN chamber. The decrease exhibited in % residue and T_d of Weeks 3 and 4 are potentially indicative of some similar degradation patterns between the units. The subsequent increase back to the original % residue and T_d observed is likely to be a result of chlorine free

radicals either crosslinking or leaving the polymer backbone to create polyacetylene moieties that lead to higher ash content.

The FT-IR spectra differences seen in **Figures 7-10** show some chemical differences in how the PVC reacted to the moisture treatment. A broad, strong peak ranging from 3200-3550 cm^{-1} , such as the one demonstrated by the Week 5 and 6 UV-exposed samples and the Week 6 xenon-exposed samples is known to be stretching of a hydroxyl group experiencing intermolecular bonding [5], usually in the form of hydrogen bonding. In this case, this is most likely water permeating into the material or the hydrolysis of chlorines in the material. However, this peak was much stronger for the UV-exposed samples than the xenon-exposed samples—dipping nearly 2% transmittance for the Week 5 and 6 UV samples, and only 0.5% for the xenon-exposed samples—and did not present at all for the Week 5 xenon sample. Thus, the deterioration of the UF PVC experienced in the UV chamber appears to make the material more able to absorb water molecules and/or hydrolyze chlorine than that of the xenon samples. This set of samples additionally exhibited a peak at 1600 cm^{-1} , which is most commonly attributed to stretching of an alkene bond [5]. This in conjunction with the higher % residue of these samples in TGA analysis indicates the presence of polyacetylene. Polyacetylene would be likely to form if radicalized chlorine leaves the polymer chain, creating unsaturation that is remedied with an alkene bond. As with the prior peak, this peak was much stronger in the UV-samples, dropping nearly 2% transmittance compared to 0.5% for the Week 6 xenon and not exhibiting a peak at all for the Week 5 xenon samples. Therefore, it is likely that the higher amount of UV wavelength photons in the QUV creates more opportunities for radicalized chlorine to form and begin the process of polyacetylene formation.

The results of the DMA also show evidence that polymer chain crosslinking occurred, more so in the UV samples. Storage modulus values beyond the glass transition temperature varied by as much as 2 GPa for the UV-exposed samples. Furthermore, the control sample was the least stiff of all samples tested and showed loss modulus behavior uncharacteristic of any other samples. Thus, the samples could be experiencing crosslinking, as chlorine radicals form through UV radiation and create radical-radical crosslinks, strengthening the material. The presence of radical-radical crosslinking also would explain why the % residue of the xenon-exposed samples that received moisture were very similar to that of the UV-exposed samples, despite not having near as strong a peak for alkene (and therefore polyacetylene moiety) presence. Nonetheless, the xenon-exposed samples exhibited storage and loss moduli that were both lower and less variable than the UV-exposed samples, showing that the amount of crosslinking present in samples in the Q-SUN may be less than those aged in the QUV.

Therefore, differences in visual appearance, chemical makeup and mechanical behavior of the PVC samples were identified, namely that the QUV shows more severe degradation in all three categories. Additional studies could investigate how much these differences manifest with further extended aging cycles (i.e. multiple thousand hours), or how these aging cycles compare to materials aged naturally in raw sunlight. Studying the different reactions other polymers commonly utilized in outdoor applications—such as high-density polyethylene—have to the different accelerated aging spectra could also be valuable. With enough data, it may be possible to determine which accelerated aging method is more representative of natural aging for a vast array of polymers designed to be exposed to the elements.

References

- [1] A. Royaux *et al.*, “Aging of plasticized polyvinyl chloride in heritage collections: The impact of conditioning and cleaning treatments,” *Polymer Degradation and Stability*, vol. 137, pp. 109–121, Mar. 2017, doi: <https://doi.org/10.1016/j.polyimdegstab.2017.01.011>.
- [2] Z. Ouyang *et al.*, “The aging behavior of polyvinyl chloride microplastics promoted by UV-activated persulfate process,” *Journal of Hazardous Materials*, vol. 424, p. 127461, Feb. 2022, doi: <https://doi.org/10.1016/j.jhazmat.2021.127461>.
- [3] P. Gijsman, J. Hennekens, and K. Janssen, “Comparison of UV degradation chemistry in accelerated (xenon) aging tests and outdoor tests (II),” *Polymer Degradation and Stability*, vol. 46, no. 1, pp. 63–74, Jan. 1994, doi: [https://doi.org/10.1016/0141-3910\(94\)90110-4](https://doi.org/10.1016/0141-3910(94)90110-4).
- [4] R. Geyer, J. R. Jambeck, and K. L. Law, “Production, use, and fate of all plastics ever made,” *Science Advances*, vol. 3, no. 7, Jul. 2017, doi: <https://doi.org/10.1126/sciadv.1700782>.
- [5] “IR Spectrum Table,” *www.sigmaaldrich.com*, 2022.
<https://www.sigmaaldrich.com/US/en/technical-documents/technical-article/analytical-chemistry/photometry-and-reflectometry/ir-spectrum-table>
- [6] E. B. Rabinovitch and J. W. Summers, “The effect of physical aging on properties of rigid polyvinyl chloride,” *Journal of Vinyl and Additive Technology*, vol. 14, no. 3, pp. 126–130, Sep. 1992, doi: <https://doi.org/10.1002/vnl.730140303>.
- [7] British Plastics Federation, “Polyvinyl Chloride PVC,” *British Plastics Federation*, 2010.
<https://www.bpf.co.uk/plastipedia/polymers/PVC.aspx>
- [8] ASTM Standard D4329, 1999, "Practice for Fluorescent UV Exposure of Plastics," ASTM International, West Conshohocken, PA, 1999, DOI: 10.1520/D4329-99.
- [9] ASTM Standard G0154, 2006, "Practice for Operating Fluorescent Light Apparatus for UV Exposure of Nonmetallic Materials," ASTM International, West Conshohocken, PA, 2006, DOI: 10.1520/G0154-06.
- [10] ASTM Standard G0155, 2005a, "Practice for Operating Xenon Arc Light Apparatus for Exposure of Non-Metallic Materials," ASTM International, West Conshohocken, PA, 2005, DOI: 10.1520/G0155-05a.
- [11] E. Yousif and R. Haddad, “Photodegradation and photostabilization of polymers, especially polystyrene: review,” *SpringerPlus*, vol. 2, no. 1, Aug. 2013, doi: <https://doi.org/10.1186/2193-1801-2-398>.